Published in final edited form as:
Cell Signal. 2011 February ; 23(2): 335–343. doi:10.1016/j.cellsig.2010.09.017.

Phospholipase D Controls *Dictyostelium* Development By Regulating G Protein Signaling

Sibnath Ray, **Yi Chen**, **Joanna Ayoung**, **Rachel Hanna**, and **Derrick Brazill***
Department of Biological Sciences, Hunter College, New York, New York 10065

Abstract

Dictyostelium discoideum cells normally exist as individual amoebae, but will enter a period of multicellular development upon starvation. The initial stages of development involve the aggregation of individual cells, using cAMP as a chemoattractant. Chemotaxis is initiated when cAMP binds to its receptor, cAR1, and activates the associated G protein, Gα2βγ. However, chemotaxis will not occur unless there is a high density of starving cells present, as measured by high levels of the secreted quorum sensing molecule, CMF. We previously demonstrated that cells lacking PldB bypass the need for CMF and can aggregate at low cell density, whereas cells overexpressing *pldB* do not aggregate even at high cell density. Here, we found that PldB controlled both cAMP chemotaxis and cell sorting. PldB was also required by CMF to regulate G protein signaling. Specifically, CMF used PldB, to regulate the dissociation of Gα2 from Gβγ. Using fluorescence resonance energy transfer (FRET), we found that along with cAMP, CMF increased the dissociation of the G protein. In fact, CMF augmented the dissociation induced by cAMP. This augmentation was lost in cells lacking PldB. PldB appears to mediate the CMF signal through the production of phosphatidic acid, as exogenously added phosphatidic acid phenocopies overexpression of *pldB*. These results suggest that phospholipase D activity is required for CMF to alter the kinetics of cAMP-induced G protein signaling.

Keywords

PLD; *Dictyostelium*; G protein; FRET; development

1. Introduction

A general principle in the development of multicellular organisms is that quorum sensing mechanisms exist that sense the density of different cell types. Often, these mechanisms use signaling molecules secreted from specific cell types. These secreted molecules activate signaling cascades which then change the developmental program of the cell. Such quorum sensing mechanisms are present in bacteria [1], *Dictyostelium discoideum* [2] and mammals [3]. The social amoeba *Dictyostelium discoideum* is the simplest eukaryote to display quorum sensing, and presents itself as an optimal organism in which to study this phenomenon. Its simple developmental cycle, and ease of biochemistry, cell biology and

*Correspondent Footnote: Hunter College, Dept. of Biological Sciences Rm 927N, 695 Park Ave, New York, NY 10065;Phone: 1(212)650-3144; Fax: 1(212)772-5227; brazill@genectr.hunter.cuny.edu.

molecular genetics makes it an excellent system in which to study eukaryotic quorum sensing. *Dictyostelium* cells exist as individual amoebae, which feed upon bacteria. When the food source runs out, and the cells begin to starve, *Dictyostelium* cells will undergo a period of differentiation and development leading to the formation of a multicellular organism. Multicellularity is initiated by the aggregation of 2×10^4 to 10^5 starving cells, using pulses of cyclic AMP (cAMP) as a chemoattractant. The aggregated cells then differentiate, and develop into a fruiting body, consisting of a mass of spore cells situated upon a column of stalk cells [4] [5]. The spores are dispersed to areas with new food sources, and eventually germinate, releasing the next generation of amoebae. However, this process will not begin unless there are sufficient numbers of starving cells present [6]. Therefore, these cells are able to sense the density of the starving cells around them and respond appropriately. Without this ability to quorum sense, small groups of cells that happen to starve at the same time would form small, ineffectual fruiting bodies.

Quorum sensing in *Dictyostelium* is accomplished by secreting and responding to a protein called Conditioned Medium Factor (CMF) [7]. CMF is an 80-kDa glycoprotein that is secreted only by starving cells [6]. When just a few cells are starving, the levels of CMF are low, and the cells are unable to enter into development. As more cells starve, the levels of CMF rise until they reach a threshold level, at which point the cells are able to initiate aggregation. Thus, cells lacking CMF are unable to aggregate, unless exogenous CMF is added [8]. Therefore, CMF appears to influence the formation of appropriate sized fruiting bodies by allowing aggregation to occur only when most of the cells in a given area are starving, as measured by high levels of CMF.

CMF exerts control over development by regulating the response to the chemoattractant cAMP during aggregation [9]. When aggregating, a *Dictyostelium* cell has a typical response to a pulse of cAMP; it releases a burst of cAMP to relay the signal to other starving cells, moves towards the source of cAMP, and activates the expression of genes involved in development [10] [11] [12] [13] [14] [15] [16]. This response is initiated by cAMP binding to the cAMP receptor [17], cAR1, which causes a transient influx of Ca^+ [18] [19] [20], and activates an associated heterotrimeric G protein. The Gα2 subunit releases GDP and binds GTP, causing it to separate from the Gβγ subunits. The freed subunits activate downstream signaling pathways required for chemotaxis and aggregation [21]. Eventually, the intrinsic GTPase activity of Gα2 hydrolyzes the GTP to GDP, allowing its reassociation with Gβγ and cAR1. However, this whole process occurs only when the cells are at high cell density, and thus in the presence of CMF. In the absence of CMF, cAMP still binds cAR1, which causes Gα2 to release GDP and bind GTP. Yet, the activation of downstream signaling is inhibited [9]. CMF accomplishes this by controlling the GTPase rate of Gα2 [22]. When CMF is absent, the GTPase rate is very high; Gα2 is rapidly converted from the active to the inactive form, and reassociates with Gβγ. Signaling is thus blocked. However, when CMF is present, the GTPase rate is low, Gα2 remains in the active, dissociated form, and signaling occurs. Thus, CMF may regulate aggregation by modulating the dissociation of Gα2 from Gβγ.

One method of measuring the dissociation of proteins is fluorescence resonance energy transfer (FRET). This type of energy transfer occurs when the emission spectrum of a donor fluorescent molecule overlaps with the excitation spectrum of an acceptor fluorescent molecule. This process is distance dependent, and typically functions when the molecules are within 10 nm of each other, a distance useful for measuring protein-protein interactions. During FRET, the donor's fluorescence intensity decreases while the acceptor's emission increases. G protein FRET has been performed in *Dictyostelium* using Gα2-CFP as a donor and Gβ-YFP as an acceptor [23] [24]. When the G protein is in the inactive, GDP-bound form, Gα2 and Gβ are complexed, and FRET can occur. When the G protein is in the active,

GTP-bound form, Gα2 and Gβ are dissociated and FRET cannot occur. Thus, this system is well-designed to study the effect of CMF on the dissociation of Gα2 from Gβγ.

We have previously demonstrated that CMF exerts its effect on cAR1 signaling by activating its own G protein signaling pathway using Gα1 and Gβ to control the activity of phospholipase C [25]. This in turn regulates the cAMP-stimulated GTPase activity of Gα2. We have also found that CMF uses the phospholipase D orthologue, PldB, to control quorum sensing [26]. In this report, we present evidence that PldB has phospholipase D activity, and regulates chemotaxis and cell sorting. In addition, using FRET, we find that CMF controls the dissociation of the G protein Gα2βγ, and that this control is dependent upon PldB.

2. Materials and methods

2.1 Cell Culture

Dictyostelium AX3 cells expressing Gα2-CFP and Gβγ-YFP (WT-FRET) and *Dictyostelium* AX3 cells lacking *pldB* and expressing Gα2-CFP and Gβγ-YFP (PLDKO-FRET) were grown in shaking culture in medium containing G418 (20 μg/ml) and G418 (20 μg/ml) plus blasticidin (10 μg/ml), respectively [26]. The WT-FRET cells were a generous gift from Dr. Janetopoulos (Vanderbilt University).

A *pldB* disruption construct was generated by replacing 719 nucleotides of the *pldB* gene with the blasticidin resistant cassette in the WT-FRET cells. 10 μg of the construct was linearized with restriction enzyme PvuI and gel purified. PLDKO-FRET cells were created by transforming purified plasmid into WT-FRET cells as described in Gaudet *et al.*. The stable tranformants were plated with the br/1 –*E. coli* strain on GYP plates containing 20 μg/ml G418 and 10 μg/ml blasticidin. Several isolates were identified and the disruption of *pldB* was confirmed PCR. The phenotypes of the isolates were also confirmed by their ability to aggregate at low cell density [26]. All FRET cells used were able to aggregate and form fruiting bodies similarly to their parental non-FRET versions.

2.2 Phospholipase D Activity Assay

Cells were incubated at 10^6 cells/ml in HL5 with [9,10-^{3}H(N)]-Palmitic Acid (Perkin Elmer, Wellesley, MA) at 5 μCi/ml in a culture dish for 24 hours at room temperature, as described previously [28]. For starvation, cells were washed with 5 ml PBM and starved in 10 ml PBM for 5 hours. Cells were then resuspended in 5 ml PBM and mixed with 5 ml PBM containing 70 μl butan-1-ol or tertiary-butanol to achieve 0.7% final concentration. The cells were then incubated at room temperature for 22 minutes. Lipids were extracted and characterized by thin layer chromatography [29]. The phosphatidylbutanol formed by PLD-catalyzed transphosphatidylation was visualized by autoradiography followed by densitometry and quantification using ImageQuant software (GE Healthcare, Piscataway, NJ). The density of the band corresponding to the tertiary-butanol reaction (background) was subtracted from that of the butan-1-ol reaction to determine PLD activity.

2.3 Chemotaxis Assay

Cells were starved by shaking in PBM at 2×10^7 cells/ml for 5 hours. All the wells of a 24-well Transwell plate (Corning, Corning, NY) were preloaded with 600 μl PBM and inserts were placed into half of the wells. 7.5×10^5 vegetative or starved cells in 100 μl PBM were loaded into each insert. After allowing the cells to settle for 10 minutes, each insert was transferred to a new well. The inserts sat for another 3 minutes, after which 6 μl 1 mM cAMP was added to half of the wells. The plate was incubated for 3 hours at 22°C. The inserts were then removed and 3 μl of 2 mM Calcein-AM (Calbiochem, San Diego, CA) was

added to all the wells and mixed gently. The plate was then incubated at room temperature in the dark for 75 minutes. The Calcein-AM was removed, the cells resuspended in fresh PBM, and their fluorescence measured (Abs/Em = 488/526) using a Typhoon scanner and quantified by ImageQuant software (GE Healthcare, Piscataway, NJ). Under agarose chemotaxis assays were performed as described in Woznica and Knecht[30]. Briefly vegetative cells were grown to log phase, collected and resuspended at 1×10^6 cells/ml. A 0.1 ml sample of the cells was placed in a trough 5 mm away from a trough with a 0.1 mM solution of folate. Cells were imaged and tracked as they moved up the folate gradient, under the agarose using Image J software as described above. Directionality is defined as the ration of (the absolute distance travel)/(the total path length). Thus, a value of 1 represents a straight path with no deviations, and decreasing values represent less efficient chemotaxis. The paired t-test was used to determine statistical significance.

2.4 Chimeras

Chimeras were created by collecting 1.0×10^7 Ax2 cells and 1.0×10^7 *pldB*$^-$ strain expressing either β-galactosidase or GFP. For β-galactosidase staining, chimeras consisting of 10% *pldB*$^-$ cells and 90% Ax2 cells were developed on white filter pads, 0.8um pore size (Millipore, Billerica, MA). Developed chimeras were then fixed and stained according to Jermyn and Williams. Pictures were taken with a dissecting microscope utilizing SPOT Advanced program with SPOT insight color camera, (Diagnostics Instruments, USA). For GFP cell localization, chimeras consisted of 5% GFP expressing *pldB*$^-$ cells and 95% Ax2 cells. Starved cells were seeded at ~2×10^5 cells/cm^2 on plastic dishes in PBM buffer. Once streams began to form, a time lapse movie was compiled by capturing an image of the cells every 10 minutes for 12 hours with an inverted Nikon TE 200 Eclipse microscope using a Metafluor Image System viewed through a 20x objective.

2.5 GTPase Assay

Cells were starved by shaking in PBM at 10^7 cells/ml for 5 hours. Cells were then washed twice with PBM and resuspended in lysis buffer [31] to 10^8 cells/ml. One set of cells was lysed immediately by passage through a 5 μm nylon filter (GE Water & Process, Trevose, PA) on ice. The other set was incubated with 1 ng/ml CMF for 30 seconds and then lysed. Membranes were assayed for the cAMP-stimulated high affinity GTPase activity associated with Gα2 as described previously [31]. The results are reported as percent increase in GTPase activity in order to normalize for differences in basal GTPase activity in different cell lines.

2.6 Expression & purification of GST-tagged recombinant Conditioned Medium Factor (GST-CMF)

To clone the CMF gene, RT-PCR was performed using the GeneAmp RNA PCR kit (Applied Biosystems, Foster City, CA) according to the manufacturer protocol, with some modification. In brief, total RNA was isolated from AX2 cells using Trizol Reagent (Invitrogen, Carlsbad, CA) as described by their protocol. RT reactions were performed using 1μg of total RNA, downstream CMF reverse primer, 5'-GTCGACTTAACAAACAGAGTTGGAACTCATTT containing a SalI restriction site and MuLV reverse transcriptase, in 20 μl volumes. The conditions for reverse transcription were 30 min at 42°C, 5 min at 99 °C and 5 min at 5 °C in a PTC-100 Peltier thermal cycler (MJ research). The PCR reactions were performed using the RT product, the upstream forward CMF primer containing a BamH1 restriction site 5'-GGATCCATGGGTTCATTTGGTATTGATG and Amplitaq DNA polymerase. The conditions were: 1) initial denaturation for 2 min at 95 °C; 2) 35 cycles of 95 °C for 1 min and 55 °C for 2 min; followed by 3) a final extension at 72 °C for 7 min. The 1.4 kb RT-PCR product was purified (Qiagen Inc, Valencia, CA), and digested with BamHI/SalI. The

purified product was ligated into the gel purified BamHI/SalI-digested expression vector pGEX-4T2. The expression construct was transformed into *Escherichia* coli BL21, and recombinant GST tagged CMF protein was expressed and purified using Glutathione Sepharose 4B beads, according to the manufacturer's protocol (GE, Piscataway, NJ). The purified protein was dialyzed against PBM (20 mM KH_2PO_4, 10 μM $CaCl_2$ and 1 mM $MgCl_2$ at pH 6.1). This GST-CMF was used in all assays requiring CMF.

2.7 Measuring FRET during CMF and cAMP stimulation

To examine the fluorescence resonance energy transfer (FRET), WT-FRET cells and PLDKO- FRET cells were cultured at density 5×10^6/ml and harvested by centrifugation at 500 g for 5 minutes. The cells were washed three times with PBM (20 mM KH_2PO_4, 10 μM $CaCl_2$ and 1 mM $MgCl_2$ at pH6.1) and resuspended at the density 2×10^7 cells/ml in the dark to avoid photo bleaching. To ensure cAMP receptor cAR1 expression, cells were starved in PBM for 2 hours with constant shaking followed by stimulation with 50 nM Adenosine 3',5'- cyclic Monophosphate, Sodium Salt (cAMP) (EMD Biosciences, Inc. Gibbstown, NJ) every six minutes interval for another 4 hours while shaking. Cells were then treated with 3 mM caffeine (Sigma Aldrich, St. Louis, MO) for 20 minutes to prevent the activation of adenylyl cyclases. Cells were washed two times with 3mM caffeine in PBM buffer and suspended in the same buffer to a density of 2×10^7 cells/ml. For each measurement, 1 ml cells were centrifuged at 500 g for 5 min and resuspended in fresh caffeine/PBM buffer. cAMP, CMF or both were added to the cells and the spectra taken. CMF was added to 1.5 ng/ml as this is the optimal CMF concentration for quorum sensing [32] [22]. cAMP was added to 100 μM based on the ability to compare our results with those previously published as well as a dose curve (data not shown). Fluorescence measurements were performed using Spex Fluorolog 2 spectrofluorometer equipped with an excitation and emission polarizer and a water cooled jacket. The cell suspension was excited at 435 nm and the emission spectrum recorded between 460 nm and 600 nm at 0.4 s/nm at 22°C. Excitation and emission slits were set at 3 nm. All wavelength spectral data were exported into Microsoft Excel and spectra were normalized to the intensity at 600 nm with respect to WT-FRET cells, and then were corrected by subtraction of a normalized wild-type (non-FRET) spectrum. The amount of FRET was determined by taking the peak intensity ratio of donor CFP and acceptor YFP at 471 nm and 525 nm respectively. For kinetic analyses, the FRET ratio was taken over the course of 110 seconds. For all other FRET measurements, the FRET ratio was measured at 10 seconds after treatment. This FRET ratio was calculated for both cell lines in the presence of buffer, cAMP, CMF and cAMP + CMF. Loss of FRET was calculated as was done by Janetopolous et al. (2001). FRET in the WT-FRET cells in the presence of buffer alone was set as 0% loss of FRET. FRET in the WT-FRET cells in the presence of cAMP was set as 100% loss of FRET. All other FRET values were placed on this scale. 20–25 individual pulse developments were performed and measured, and significance determined by pair sample t-test.

2.8 Low Cell Density Aggregation Assay

Vegetative cells were collected and washed with PBM. They were then starved as submerged monolayer culture at surface densities of 224×10^3, 112×10^3, 56×10^3, 28×10^3, 14×10^3, and 7×10^3 cells/cm^2 in 400 μl PBM, PBM supplemented with 5 μM, 25 μM, or 50 μM cell permeable phosphatidic acid, 1,2-Dioctanoyl-*sn*-Glycero-3-Phosphate (Avanti, Alabaster, AL).

3. Results

3.1 *pldB* codes for a phospholipase D

PldB, a putative PLD orthologue, was previously demonstrated to mediate quorum sensing and negatively regulate aggregation in *Dictyostelium discoideum* [26]. At that time, it was unclear whether *pldB* coded for an active PLD. A PLD enzyme is characterized by its ability to hydrolyze phosphatidylcholine to form phosphatidic acid and choline, via a phospholipid transphosphatidylation reaction. To determine whether *pldB* encodes an enzyme with phospholipase D activity, we examined the overall PLD activity in wild-type, $pldB^{-}$ and $pldB^{OE}$ cells using the standard *in vivo* transphosphatidylation assay commonly used to measure PLD activity. Using this assay, Zouwail et al. had previously demonstrated that *D. discoideum* has a basal level of PLD activity [28]. In agreement with this, we found that 5 hr starved wild-type cells are able to carry out a transphosphatidylation reaction as evidenced by the creation of phosphatidylbutanol, when given butan-1-ol as a substrate (Fig. 1A). The fact that a corresponding product was absent when the cells were given tertiary-butanol suggests that the activity was due to a PLD enzyme, as tertiary-butanol is not a preferred substrate for PLD. Cells lacking PldB had approximately 50% less PLD activity than wild-type cells, whereas cells overproducing PldB had 50% more PLD activity (Fig. 1B). The data demonstrated that loss of PldB caused an overall decrease in cellular PLD activity while overproduction of PldB caused an overall increase in cellular PLD activity, strongly suggesting that *pldB* codes for an active PLD.

3.2 PldB regulates cAMP chemotaxis

We have previously shown that PldB also seems to be involved in the timing of development, as $pldB^{-}$ cells are able to aggregate several hours ahead of wild-type cells. This could be explained by the fact that the cAMP receptor, cAR1, was expressed earlier and at higher levels in $pldB^{-}$ cells than wild-type cells [26]. However, altered chemotaxis can also result in rapid development. To test this possibility, we performed a Transwell chemotaxis assay of wild-type, $pldB^{-}$ and *pldB* overexpressing cells to the extracellular chemoattractant cAMP. Cells were allowed to migrate through an 8 μm pore membrane into a cAMP-containing well. The chemotactic index is defined as the ratio of the number of cells migrating to cAMP to the number of cells migrating to buffer. Therefore, a chemotactic index of 1 indicates that an equal number of cells moved to the cAMP as moved to the buffer, signifying no chemotaxis to cAMP. A chemotactic index larger than 1 indicates that more cells moved to the cAMP compared to buffer, representing chemotaxis to cAMP. Under vegetative conditions, wild-type, $pldB^{-}$ and $pldB^{OE}$ cells all had a chemotactic index around 1 (Fig. 2A), indicating that there was no chemotaxis to cAMP. This is in accordance with the fact that vegetative cells live as individual amoebae and are not responsive to cAMP. When cells were starved for 5 hours, wild-type and $pldB^{-}$ cells showed similar chemotactic indices of around 2, indicating that there was chemotaxis toward cAMP. However, $pldB^{OE}$ cells still had a chemotactic index near 1, denoting no chemotaxis to cAMP. The similarity in chemotactic ability between wild-type and $pldB^{-}$ cells suggests that the rapid aggregation of $pldB^{-}$ cells is not caused by an increased rate of chemotaxis or a sensitivity to cAMP in the vegetative state. However, overexpression of *pldB* blocks cAMP chemotaxis.

To examine in more detail how overexpression of *pldB* influences cAMP chemotaxis, we measured the speed and directionality of cells in a chemotactic gradient using an under agarose chemotaxis assay. In this assay, cells move up a stable cAMP gradient by crawling underneath a thin layer of agarose. Consistent with previous results, wild type Ax2 cells move towards the cAMP source with an average speed of 12 μm/min (Fig. 2B). Cells overexpressing *pldB* moved at a slightly slower 8 μm/min. Interestingly, cells

overexpressing *pldB* had a drastically reduced directionality. Directionality is a measure of the deviation of the cell movement from a straight path. Thus, cells that make a straight path have the maximal directionality of 1. Cells that perform a random walk and end up back at their starting point will have the minimal directionality of 0. Wild-type Ax2 cells had a directionality of 0.68, while cells overexpressing *pldB* had a directionality 0.10 (Fig. 2C). Thus, while cells overexpressing *pldB* have a relatively normal speed, they are unable to efficiently move up a cAMP gradient. This defect is most likely responsible for their low chemotactic index observed previously.

3.3 Cells lacking PldB preferentially sort to the stalk

We previously demonstrated that cells lacking PldB formed slightly longer stalks than normal [26]. This suggested a potential defect in cell sorting or differentiation. To investigate a role for PldB in differentiation and morphogenesis, we examined the location of *pldB*$^{-}$ cells in chimeric fruiting bodies with wild-type cells. Wild-type cells and *pldB*$^{-}$ cells expressing bgalactosidase were mixed at a ratio of 90:10 and allowed to develop. We found that cells lacking *pldB* were preferentially sorted into the stalk and cups of the final fruiting body, suggesting that cells lacking PldB had a preference for stalk cell differentiation (Fig. 3A). To ensure that loss of PldB, and not expression of β-galactosidase, was causing the preference for stalk cell differentiation, wild-type cells expressing β-galactosidase were mixed with wild-type cells. In this case, the β-galactosidase expressing cells were seen throughout the fruiting body, arguing the expression of β-galactosidase does not influence differentiation (Fig. 3B). To determine at what point during development *pldB*$^{-}$ cells first display a preference for stalk cell differentiation, we examined the location of *pldB*$^{-}$ cells when mixed with wild-type cells during aggregation. Wild-type cells and *pldB*$^{-}$ cells expressing GFP were mixed at a ratio of 95:5 and allowed to form aggregates in submerged culture. We found that initially, the *pldB*$^{-}$:GFP cells are evenly distributed in the aggregation field (Fig. 4A) and the initial mound (Fig. 4B). However, as the mound began to mature, the *pldB*$^{-}$:GFP cells began to associate with each other (Fig. 4C) and eventually ended up at the top of the mound (Fig. 4D, E, F), which is normally where prestalk cells are located. To ensure that loss of PldB and not expression of GFP was causing the localization, wild-type cells expressing GFP were mixed with wild-type cells. In this case, the GFP expressing cells were seen throughout the mound, arguing that expression of GFP does not influence differentiation (Fig. 4G, H). Thus, it appears that the preference for stalk cell differentiation exhibited by *pldB*$^{-}$ cells is first observed during mound formation, when prestalk and prespore differentiation begins.

3.4 PldB Mediates Quorum Sensing in the CMF Pathway

We had previously found that CMF regulates quorum sensing by maintaining Gα2 in the active GTP-bound state [22]. This is accomplished by decreasing the GTPase activity of Gα2 without changing its GTP binding activity [9] [22]. To examine whether CMF requires PldB to decrease the GTPase activity of Gα2, we measured the cAMP-stimulated high-affinity GTPase activity in membranes, which has been shown to be due to Gα2 [22]. In agreement with previous results, cAMP caused an approximate 30% increase in the high affinity GTPase activity associated with Gα2 in wild-type cells (Fig. 5) [22]. Addition of CMF decreased this to approximately 12%. Membranes isolated from cells lacking PldB were insensitive to CMF, as addition of CMF had no effect on the cAMP-stimulated GTPase activity of Gα2. Therefore, in membranes lacking PldB, the GTPase activity of Gα2 had been uncoupled from CMF regulation. This supports the idea that PldB is a component of the CMF-mediated quorum sensing pathway, which regulates the cAMP-stimulated GTPase activity of Gα2.

3.5 CMF increases the dissociation of Gα2βγ in the absence of cAMP

Given that CMF regulates chemotaxis by controlling G protein signaling through the cAMP chemoattractant receptor, cAR1 [9], and requires PldB for this regulation, we decided to delineate this relationship by studying the dynamics of the G protein associated with cAR1, Gα2βγ. Specifically, we focused on G-protein dissociation, by observing the changes in fluorescence resonance energy transfer (FRET) of Gα2-CFP:Gβγ-YFP complexes in WT-FRET cells. An increase in the ratio of donor fluorescence (Gα2-CFP at 471 nm) to acceptor fluorescence (Gβγ-YFP at 525 nm) is an indicator of G-protein dissociation. To determine the efficiency of our system, we first measured the change in FRET ratio when the cells were stimulated with cAMP. In accordance with previous results, we found that activation of cAR1 with 100 μM cAMP caused loss of FRET as demonstrated by an increase in emission at 471 nm and decrease in emission at 525 nm (Fig. 6). This caused an increase in the FRET ratio (471 nm/525 nm) of 23%, which is slightly less than the increase of 32% that Janetopoulos et al. [23] observed. The change in the FRET ratio suggests that the cAR1-associated Gα2βγ complexes dissociate in the presence of external cAMP.

Previous studies suggest that CMF modulates cAMP signal transduction by regulating the dynamics of Gα2-βγ interactions [32] [22]. To examine whether this is through controlling the dissociation of Gα2βγ, we examined the change in FRET associated with treatment of CMF. We found that addition of 1.5 ng/ml recombinant CMF, caused a loss of FRET roughly 61% of that seen with addition of cAMP alone (Fig. 7). This suggests that CMF, in the absence of cAMP, can cause the dissociation of Gα2βγ.

3.6 CMF augments the cAMP induced dissociation of Gα2βγ

Given that CMF can induce the dissociation of Gα2βγ in the absence of cAMP, we wanted to determine whether CMF-induced dissociation is additive with cAMP-induced dissociation. To examine this, WT-FRET cells were incubated with CMF (1.5 ng/ml) for 2 min, and the change in FRET was measured after addition of 100 μM cAMP. Addition of CMF led to an additional 22% loss of FRET over cAMP alone (Fig. 7). This increase is statistically significant ($p<0.005$), suggesting that the effect of CMF is additive with cAMP in dissociating the Gα2βγ complexes. Interestingly, this represents an increase of the 471 nm/525 nm ratio by 28%, which is comparable to the results reported by Janetopoulos et al. (2001).

3.7 PldB regulates the dissociation of Gα2βγ

We had previously found that PldB mediates CMF-based quorum sensing, in that loss of PldB allows aggregation at low cell density, mimicking the effect CMF. However, it was unclear as to how PldB was performing this function. To determine, whether PldB is involved in regulating the dissociation of Gα2βγ complexes, we examined changes in FRET associated with loss of PldB by creating PLDKO-FRET cells. Simply by disrupting the *pldB* gene, we observed a loss of FRET equal to 33% of that seen when WT-FRET cells are exposed to cAMP (Fig. 7). This suggests that PldB can regulate the dissociation Gα2βγ.

3.8 CMF regulates Gα2Gβγ dissociation through PldB

Given that both CMF and PldB control Gα2βγ dissociation, we decided to examine whether they work through the same pathway. To investigate this possibility, we compared the changes in the loss of FRET of PLDKO-FRET cells in absence and presence of CMF. Unlike in the WT-FRET cells, addition of CMF to the PLDKO-FRET cells did not induce a significant ($p>0.05$) loss of FRET (Fig. 7). A similar result was found when we examined the loss of FRET in PLDKO-FRET cells treated with cAMP in presence and absence of CMF. In stark contrast to the WT-FRET cells, CMF did not significantly augment ($p>0.05$)

the loss of FRET in PLDKO-FRET cells. These data suggest that CMF requires PldB in order to regulate the dissociation of Gα2βγ.

3.9 Loss of PldB mimics the presence of CMF in cells treated with cAMP

Since the loss of PldB mimics the addition of CMF by allowing aggregation at low cell density [26], we decided to examine whether the loss PldB can mimic the change in FRET associated with CMF in the presence of cAMP. We found that the PLDKO-FRET cells treated with cAMP alone had a larger loss of FRET than that seen when WT-FRET cells are exposed to cAMP (Fig. 7). This was similar to the loss of FRET seen in WT-FRET cells in presence of CMF and cAMP. Thus, there is no significant difference ($p>0.05$) in the loss of FRET observed during cAMP signaling between WT-FRET cells pretreated with CMF and untreated PLDKO-FRET cells. This suggests that loss of PldB mimics the effect of CMF in cells treated with cAMP.

3.10 PldB regulates CMF signalling through production of phosphatidic acid

The principal PLD activity in all organisms studied to date is the hydrolysis of phosphatidylcholine to produce phosphatidic acid and choline. Since phosphatidic acid is a known signaling molecule in eucaryotic cells, it is very likely that PldB uses phosphatidic acid to mediate CMF signaling. To determine whether phosphatidic acid serves as a downstream messenger of PldB in quorum sensing pathways, we performed low cell density aggregation assays in the presence and absence of exogenously added phosphatidic acid. As seen previously, wild-type cells are able to aggregate down to a density of 28×10^3 cells/cm2, whereas *pldB*$^-$ cells aggregate down to 7×10^3 cells/cm2 (Table 1) [26]. Addition of cell permeable phosphatidic acid to 5 mM inhibited aggregation in both wild-type and *pldB*$^-$ cells, with wild-type cells being more sensitive to added phosphatidic acid than *pldB*$^-$ cells. Addition of phosphatidic acid to 25 mM had an even greater effect, and addition to 50 mM completely blocked aggregation, even at the highest concentration of cells. Thus, addition of phosphatidic acid at this concentration phenocopies overexpression of *pldB* [26]. This implicates phosphatidic acid as a downstream signal of PldB in the CMF quorum sensing pathway.

4. Discussion

4.1 PldB is a phospholipase D

Three PLD1 orthologs have been predicted from the *Dictyostelium* genome, PldA, PldB, and PldC [33] [34]. While Zouwail et al. demonstrated through butanol inhibition that PLD activity is required for cell motility and proper F-actin organization [28], the enzymatic activity of these proteins has not been monitored. We have examined the role of PldB in PLD activity, and found that cells lacking PldB have decreased PLD activity, and cells overproducing PldB have increased PLD activity. While the change in PLD activity could be an indirect effect, this possibility is unlikely. Given the fact that PldB contains all of the conserved domains found in PLD enzymes, and given its sequence similarity to mammalian PLD1, the more likely interpretation of these results is that PldB is a true phospholipase D. We also find that the loss of PldB does not remove all PLD activity from cell lysates. In 5 hour starved cells, PldB accounts for approximately 50% of the total PLD activity. Presumably, the remaining PLD activity seen in the *pldB*$^-$ cells comes from PldA and/or PldC.

4.2 PldB controls cell sorting

Cells lacking PldB preferentially sort to the stalk. This appears to begin during mound formation, as *pldB*$^-$ cells begin to sort out to the tip of chimeric mounds. This is the area of

the mound normally populated by prestalk cells. Cells can sort based on differential speed and differential adhesion [35] [36] [37]. Here we show that PldB can regulate chemotaxis to cAMP, suggesting that *pldB*$^{-}$ cells may have a different speed. Others have also shown that PLD activity is involved in regulating speed. Zouwail et al. showed that inhibition of PLD activity with ethanol causes disruption of actin based motility [28]. A specific role for PldB in motility was also demonstrated by Nagasaki and Uyeda when they saw that cells lacking PldB had decreased motility compared to wild-type cells [38]. Both mathematical modeling and experimental evidence have shown that differential adhesion can lead to differential sorting [37] [39] [40]. Specifically, more adhesive cells sort to the prestalk zone [41]. Interestingly, PldB may also be implicated in adhesion. We have seen that cells lacking PldB are more adherent to each other than wild-type cells (unpublished data). So, the altered adhesion and or motility seen in the *pldB*$^{-}$ cells could explain why they preferentially sort to the tip of the mound and eventually become stalk cells.

4.3 PldB mediates CMF-based quorum sensing by regulating the dynamics of G protein signaling

While it was known that PldB was involved in quorum sensing by CMF, the nature of this relationship remained unclear [26]. It was postulated that CMF controlled chemotactic signal transduction through the cAMP receptor, cAR1 [9], and that CMF acted through the regulation of the G protein associated with cAR1 [22], Gα2. It had been established that CMF signaling had no effect on the interaction between cAR1 and its associated G protein, as CMF did not influence GTP binding to Gα2 in response to cAMP [9][22]. In fact, CMF was shown to specifically regulate the GTPase activity of Gα2 in response to cAMP [22] [25]. However, a link between PldB and Gα2 remained elusive. We now find that CMF requires PldB to regulate the GTPase activity of Gα2. However, this, and previous findings were derived from studies restricted to membrane preparations and the artifacts associated with cell fractionation. Thus, the mechanism of PldB and CMF action remained undefined due to technical limitations. These limitations have been abolished with the advent of FRET in live cells. By tagging the components of G-proteins with fluorescent proteins, their interactions can be measured in living cells [24]. Using this system in *Dictyostelium discoideum*, it had been shown that when cAMP is not bound to the cAR1 receptor, Gα2, Gβ and Gγ form a heterotrimer, as evidenced by FRET between the YFP-labeled Gα2 and the CFP labeled Gβ [23]. When cAMP binds the receptor, Gα2 releases GDP and binds GTP. The heterotrimer then dissociates, as measured by a loss of FRET. We have duplicated these findings and found that the amount of FRET is not only dependent upon the presence of cAMP, but also upon the presence of CMF. We found that CMF alone causes a loss of FRET. This could be explained in at least three ways. It could be that CMF is activating the G protein directly. Activation of the G protein by CMF would necessitate Gα2 binding GTP, causing an increase in the amount of GTP binding to membranes. However, previous experiments showed that addition of CMF had no significant effect on the amount of GTP binding to membranes [9] [22]. Therefore, direct activation of the G protein by CMF seems unlikely.

Another possibility is that CMF is inducing a conformational change in the G protein whereby the CFP and YFP attached to Gβ and Gα2, respectively, are moving away from each other without the G protein heterotrimer separating. FRET only works over a distance of less than 10 nm. Thus, if CMF causes a conformational change in the heterotrimer whereby CFP and YFP are separated by more than 10 nm, there could be a loss in FRET. Such a possibility cannot be completely ruled out [42], but is unlikely. In addition to observing that cAMP or CMF alone causes a loss of FRET, we found that CMF significantly augments the loss of FRET seen by addition of cAMP. The dose of cAMP that we are giving the cells is in great excess to CMF. It has been calculated that under our conditions, roughly

200 molecules of CMF are bound to a cell, compared to 20,000 molecules of cAMP [43]. If CMF were simply causing the YFP to move away from the CFP, we wouldn't expect CMF to have a large effect on FRET, as the addition of cAMP would already have dissociated the G protein. Thus, such a significant effect on FRET by such a small amount of CMF could not easily be explained by a slight conformational change in the G protein.

The third possibility is that CMF affects the steady state levels of activated and resting G proteins. G protein signaling is balanced between the inactive Gαβγ heterotrimer and the active Gα and Gβγ subunits [42]. Proteins can modify this cycle by increasing GTP binding, as receptors do, or by increasing GTP hydrolysis, as GTPase activating proteins do. Previous work suggested that CMF regulates the cycle by decreasing the GTPase activity of Gα2, thus increasing the time during which the G protein is dissociated [22]. However, this work was done in fractionated cells and did not look specifically at the activity of Gα2. Our work presented here overcomes these limitations by working with whole cells and looking directly at the dissociation of Gα2 from Gβγ. The loss of FRET that we see with the addition of CMF suggests that CMF prolongs the amount of time that the G protein is in the dissociated, active form. In addition, the ability of CMF to augment the loss of FRET seen with cAMP is also explained by this. If CMF is decreasing the GTPase activity of Gα2, the cAMP will stimulate G protein dissociation, and the CMF will prolong the amount of time the G protein remains dissociated, thus increasing the loss of FRET.

Here we present evidence that PldB is involved in transducing the CMF signal that regulates Gα2 and Gβγ dissociation. To further elucidate the role of PldB in regulating Gα2, we performed FRET experiments on cells lacking PldB. We found that CMF had no significant effect on cells lacking PldB. By losing PldB, the CMF signaling pathway to Gα2 had been disrupted. This loss of signaling corroborates our GTPase assays. As mentioned previously, in wild type cells, CMF causes a decrease in the cAMP-stimulated GTPase activity associated with Gα2 [22]. Much like the FRET experiments, cells lacking PldB no longer exhibit a CMF effect. Interestingly, cells lacking PldB had a loss of FRET similar to cells in the presence of CMF. Thus, the CMF signaling pathway appears to be stuck in the “on” position. This is also in keeping with previous results which showed that cells lacking PldB are able to aggregate at lower cell densities than wild-type cells can [26]. In other words, even when cells lacking PldB are at too low a density to accumulate CMF, they are able to aggregate because the CMF pathway has been artificially activated by the loss of PldB.

Our research suggests that phosphatidic acid, the product of PLD activity, may link PldB to the regulation of Gα2 by CMF. We see that addition of phosphatidic acid is able to mimic overexpression of *pldB* in our low cell density aggregation assay, suggesting that the reason *pldB* overexpressing cells are not able to quorum sense is because they have overproduced phosphatidic acid. In support of this interpretation, we find that cells lacking PldB are more resistant to the effects of phosphatidic acid in this assay. This is easily explained by the fact that cells lacking PldB would have less cellular phosphatidic acid to begin with when compared to wild-type cells. Thus, it would take more exogenous phosphatidic acid to inhibit quorum sensing. These results argue strongly that PldB is mediating quorum sensing through its production of phosphatidic acid.

Taken together, these results support the following model (Fig. 9). Under low cell density conditions, CMF levels are low. Consequently, PldB activity, and thus phosphatidic acid levels, are high, supporting association between Gα2 and Gβγ. This decreases cAMP signaling, preventing aggregation and development. As more cells begin to starve, the levels of CMF increase until they reach a threshold level. At this point, CMF activates its receptor. This signaling leads to the inhibition PldB, and a corresponding decrease in cellular phosphatidic acid levels, thus supporting the dissociation of Gα2 from Gβγ by regulating the

GTPase activity of Gα2. This increases cAMP signaling, allowing chemotaxis and aggregation to occur.

At least one phospholipase D gene has been identified in all animals studied to date. Recently, PLDs in lower eukaryotes have been identified and are beginning to be studied. PLD genes have been found in *A. nidulans*, *C. albicans*, and *S. cerevisiae* [44] [45] [46]. In all cases, PLD has been associated with development. In *A. nidulans*, PLD activity spikes shortly after germination, during hyphal growth [44]. In *C. albicans*, PLD is required for virulence and hyphae formation [47] [48]. In *S. cerevisiae*, PLD is essential to mating and sporulation [49]. Thus, it is not surprising that in *Dictyostelium* PLD plays a role in both quorum sensing and differentiation.

5. Conclusion

These findings provide evidence that the phospholipase D orthologue, PldB, performs at least two functions during *Dictyostelium* development. First, it mediates CMF-dependent quorum sensing by regulating cAMP signaling through controlling the dissociation of the G protein associated with the cAMP receptor, cAR1. Second, it controls differentiation in the fruiting body, most likely by its control of cell sorting in the mound.

Acknowledgments

We thank Christopher Janetopoulos for the wild-type cells expressing Gα2-CFP and Gβγ-YFP (WT-FRET). This publication was made possible by grant S06-GM606564 from the National Institutes of Health, grant 0346975 from the National Science Foundation, and grant RR03037 from the National Center for Research Resources (NCRR), a component of the National Institutes of Health (NIH). Its contents are solely the responsibility of the authors and do not necessarily represent the official views of NCRR or NIH.

References

1. Gomer RH. Knowing that you're among friends. Curr. Biol 1994;4:734–735. [PubMed: 7953564]
2. Clarke M, Gomer RH. PSF and CMF, autocrine factors that regulate gene expression during growth and early development of Dictyostelium. Experientia 1995;51:1124–1134. [PubMed: 8536800]
3. Zhang Y, Ricardo P. Positional cloning of the mouse obese gene and its human homologue. Nature 1994;372:425–432. [PubMed: 7984236]
4. Kessin, RH. Dictyostelium - Evolution, cell biology, and the development of multicellularity. Cambridge Univ. Press; Cambridge, UK: 2001. p. xivp. 294
5. Loomis, WF. Dictyostelium discoideum. A developmental system. Ac. Press; New York: 1975. p. 214
6. Gomer RH, Yuen IS, Firtel RA. A secreted 80×10(3)Mr protein mediates sensing of cell density and the onset of development in Dictyostelium. Development 1991;112:269–278. [PubMed: 1663029]
7. Mehdy MC, Firtel RA. A secreted factor and cyclic AMP jointly regulate cell-type-specific gene expression in Dictyostelium discoideum. Mol. Cell. Biol 1985;5:705–713. [PubMed: 2985966]
8. Jain R, et al. A density-sensing factor controls development in Dictyostelium. Genes Devel 1992;6:390–400. [PubMed: 1547939]
9. Yuen IS, et al. A density-sensing factor regulates signal transduction in Dictyostelium. J. Cell Biol 1995;129:1251–1262. [PubMed: 7775572]
10. Devreotes P. Dictyostelium discoideum: a model system for cell-cell interactions in development. Science 1989;245:1054–1058. [PubMed: 2672337]
11. Firtel RA, et al. G protein linked signal transduction pathways in development: Dictyostelium as an experimental system. Cell 1989;58:235–239. [PubMed: 2546676]
12. Dottin RP, et al. Signal transduction and gene expression in Dictyostelium discoideum. Dev. Genet 1991;12:2–5. [PubMed: 2049877]

13. Firtel RA. Integration of signaling information in controlling cell-fate decisions in Dictyostelium. Genes Devel 1995;9:1427–1444. [PubMed: 7601348]
14. Gross JD. Developmental decisions in Dictyostelium discoideum. Microbiol. Rev 1994;58:330–351. [PubMed: 7968918]
15. Peters DJM, et al. Control of cAMP-induced gene expression by divergent signal transduction pathways. Dev. Genet 1991;12:25–34. [PubMed: 1646693]
16. Schaap, P. Intercellular interactions during Dictyostelium development. In: Dworkin, M., editor. Microbial Cell-Cell Interactions. Am. Soc. Microbiol.; Washington, DC: 1991. p. 147-178.
17. Theibert A, Devreotes P. Surface receptor-mediated activation of adenylate cyclase in Dictyostelium. Regulation by guanine nucleotides in wild-type cells and aggregation deficient mutants. J. Biol. Chem 1986;261:15121–15125. [PubMed: 3771567]
18. Bumann J, Wurster B, Malchow D. Attractant-induced changes and oscillations of the extracellular Ca++ concentration in suspensions of differentiating Dictyostelium cells. J. Cell Biol 1984;98:173–178. [PubMed: 6323484]
19. Milne JL, Coukell MB. A Ca2+ transport system associated with the plasma membrane of Dictyostelium discoideum is activated by different chemoattractant receptors. J. Cell Biol 1991;112:103–110. [PubMed: 1986000]
20. Milne JL, Devreotes PN. The surface cyclic AMP receptors, cAR1, cAR2, and cAR3, promote Ca2+ influx in Dictyostelium discoideum by a Galpha2-independent mechanism. Mol. Biol. Cell 1993;4:283–292. [PubMed: 8485319]
21. Sasaki AT, Firtel RA. Regulation of chemotaxis by the orchestrated activation of Ras, PI3K, and TOR. Eur. J. Cell Biol 2006;85:873–895. [PubMed: 16740339]
22. Brazill DT, Gundersen R, Gomer RH. A cell-density sensing factor regulates the lifetime of a chemoattractant-induced Galpha-GTP conformation. FEBS Lett 1997;404:100–104. [PubMed: 9074646]
23. Janetopoulos C, Jin T, Devreotes P. Receptor-mediated activation of heterotrimeric G-proteins in living cells. Science 2001;291:2408–2411. [PubMed: 11264536]
24. Janetopoulos C, Devreotes P. Monitoring receptor-mediated activation of heterotrimeric G-proteins by fluorescence resonance energy transfer. Methods 2002;27:366–373. [PubMed: 12217653]
25. Brazill DT, et al. Cell density sensing mediated by a G protein-coupled receptor activating phospholipase C. J. Biol. Chem 1998;273:8161–8168. [PubMed: 9525920]
26. Chen Y, et al. PldB, a putative phospholipase D homologue in Dictyostelium discoideum mediates quorum sensing during development. Euk. Cell 2005;4:694–702.
27. Gaudet P, et al. Transformation of Dictyostelium discoideum with plasmid DNA. Nature Protocols 2007;2:1317–1324.
28. Zouwail S, et al. Phospholipase D activity is essential for actin localization and actin-based motility in Dictyostelium. Biochem. J 2005;389:207–214. [PubMed: 15769249]
29. Song JG, Pfeffer LM, Foster DA. v-Src increases diacylglycerol levels via a type D phospholipase-mediated hydrolysis of phosphatidylcholine. Mol Cell Biol 1991;11:4903–4908. [PubMed: 1656217]
30. Woznica D, Knecht DA. Under-agarose chemotaxis of Dictyostelium discoideum. Meth. Mol. Biol 2006;346:311–325.
31. Snaar-Jagalska BE, Jakobs KH, van Haastert PJM. Agonist-stimulated high-affinity GTPase in Dictyostelium membranes. FEBS Lett 1988;236:139–144. [PubMed: 2841161]
32. Deery WJ, et al. A single cell density-sensing factor stimulates distinct signal transduction pathways through two different receptors. J. Biol. Chem 2002;277:31972–31979. [PubMed: 12070170]
33. Eichinger L, et al. The genome of the social amoeba Dictyostelium discoideum. Nature 2005;435:43–57. [PubMed: 15875012]
34. Chisholm RL, et al. dictyBase, the model organism database for Dictyostelium discoideum. Nucl. Acids Res 2006;34:D423–D427. [PubMed: 16381903]
35. Vasiev B, Weijer CJ. Modeling chemotactic cell sorting during Dictyostelium discoideum mound formation. Biophys. J 1999;76:595–605. [PubMed: 9929466]

36. Palsson E. A 3-D model used to explore how cell adhesion and stiffness affect cell sorting and movement in multicellular systems. J Theor Biol 2008;7:1–13. [PubMed: 18582903]
37. Maree AFM, Panfilov AV, Hogeweg P. Migration and thermotaxis of Dictyostelium discoideum slugs, a model study. J. Theor. Biol 1999;199:297–309. [PubMed: 10433894]
38. Nagasaki A, Uyeda TQ. Screening of genes involved in cell migration in Dictyostelium. Exp. Cell Res 2007;314:1136–1146. [PubMed: 18164290]
39. Maree AFM, Hogeweg P. How amoeboids self-organize into a fruiting body: multicellular coordination in Dictyostelium discoideum. Proc. Natl. Acad. Sci. USA 2001:3879–3883. [PubMed: 11274408]
40. Jiang Y, Levine H, Glazier J. Possible cooperation of differential adhesion and chemotaxis in mound formation of Dictyostelium. Biophys. J 1998;75:2615–2625. [PubMed: 9826586]
41. Queller DC, et al. Single-gene greenbeard effects in the social amoeba Dictyostelium discoideum. Science 2003;299:105–106. [PubMed: 12511650]
42. Lambert N. Dissociation of Heterotrimeric G proteins in Cells. Sci. Signal 2008;1(25):re5. [PubMed: 18577758]
43. van Haastert PJM, Bishop JD, Gomer RH. The cell density factor CMF regulates the chemoattractant receptor cAR1 in Dictyostelium. J. Cell Biol 1996;134:1543–1549. [PubMed: 8830781]
44. Hong S, Horiuchi H, Ohta A. Molecular cloning of a phospholipase D gene from Aspergillus nidulans and characterization of its deletion mutants. FEMS Microbiol Lett 2003;224:231–237. [PubMed: 12892887]
45. Kanoh H, et al. Molecular cloning of a gene encoding phospholipase D from the pathogenic and dimorphic fungus, Candida albicans. Biochim Biophys Acta 1998;1398:359–364. [PubMed: 9655935]
46. Waksman M, et al. Identification and characterization of a gene encoding phospholipase D activity in yeast. J Biol Chem 1996;271:2361–2364. [PubMed: 8576189]
47. Dolan JW, et al. Candida albicans PLD I activity is required for full virulence. Med Mycol 2004;42:439–447. [PubMed: 15552646]
48. Hube B, et al. The role and relevance of phospholipase D1 during growth and dimorphism of Candida albicans. Microbiology 2001;147:879–889. [PubMed: 11283284]
49. Ella KM, et al. Characterization of Saccharomyces cerevisiae deficient in expression of phospholipase D. Biochem J 1996;314:15–19. [PubMed: 8660276]

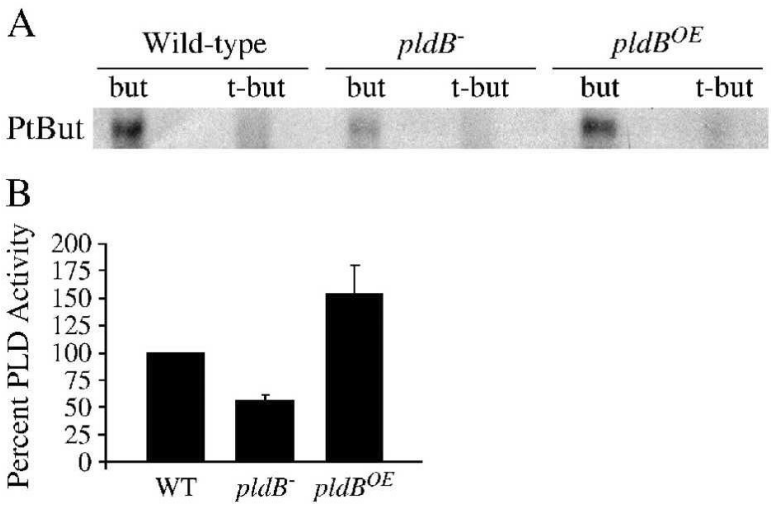

Fig 1.

Cellular PLD activity. *In vivo* transphosphatidylation assays were performed using butanol as a substrate. Lipids were extracted, separated by thin layer chromatography, exposed to film, and the bands measured by densitometry. Tertiary-butanol was used as a negative control. (A) Representative radiography from starved samples. (B) Densitometry results from starved cells from 5 independent experiments ± SEM.

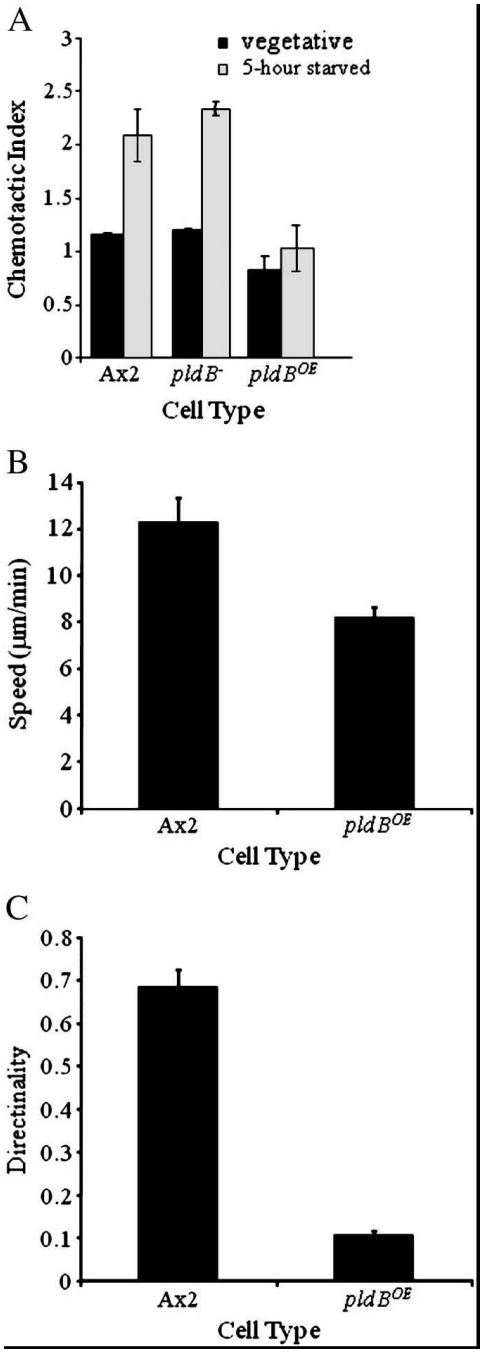

Fig2.

Chemotaxis towards cAMP. (A) Vegetative and 5-hour starved Ax2, *pldB*$^{-}$ and *pldB*^{OE} cells were placed in a transwell plate and allowed to migrate through the pores towards buffer or cAMP. Chemotactic index = (cells migrated towards cAMP)/(cells migrated towards buffer). Starved Ax2 and *pldB*^{OE} cells were placed in a cAMP gradient and their (B) speed and (C) directionality measured. The results are the average of three experiments +/− SEM.

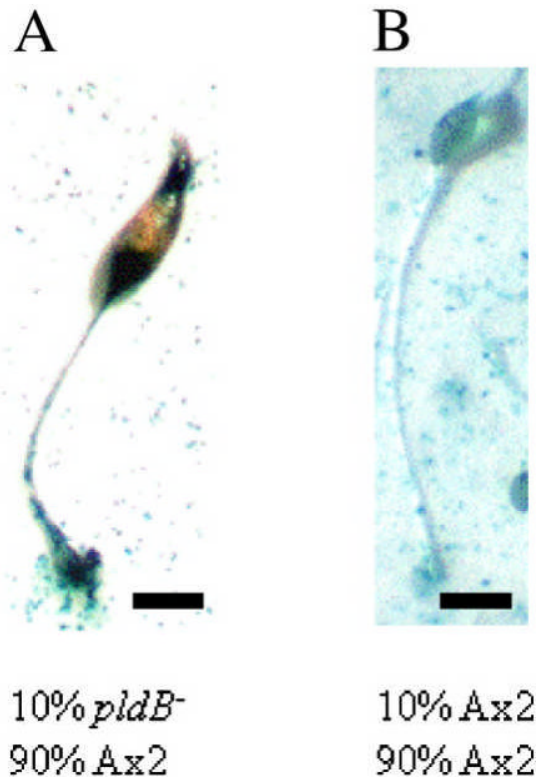

Fig 3.

Chimeric fruiting bodies stained for β-galactosidase. Chimeric fruiting bodies consisting of (A) 90% Ax2 and 10% *pldB*$^{-}$: β-gal cells or (B) 90% Ax2 and 10% Ax2: β-gal cells were fixed and stained with X-GAL. Bars 0.5 mm.

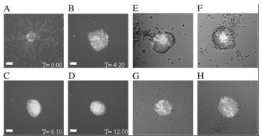

FIG 4.

Chimeric aggregates. Ax2 and *pldB*$^{-}$:GFP cells were mixed at a ratio of 95:5 and allowed to form aggregation fields in submerged culture. A time lapse film was created by taking photos every 20 minutes for 12 hours. Photos represent (A) initial aggregation field, (B) initial aggregate, (C) maturing aggregate and (D) final mound. The time associated with each photo is presented. (E, F) Photos representing 2 separate mounds of Ax2 and *pldB*$^{-}$:GFP cells mixed at a ratio of 95:5. (G, H) Ax2 cells and Ax2:GFP cells were mixed at a ratio of 95:5 and allowed to form mounds in submerged culture. Bars 2 mm.

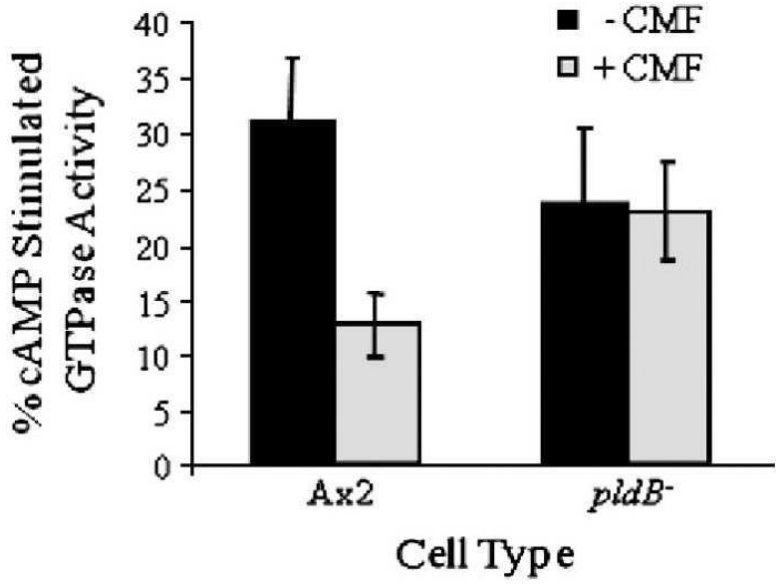

FIG 5.

The effect of CMF on cAMP-stimulated high affinity GTPase. Wild-type and *pldB*$^{-}$ cells were starved and treated either with buffer or recombinant CMF. 30 seconds later, the cells were lysed, and the membranes isolated and then treated with cAMP. They were then assayed for the ability to hydrolyze [γ-^{32}P]GTP. The results are the means of 5 experiments ± SEM.

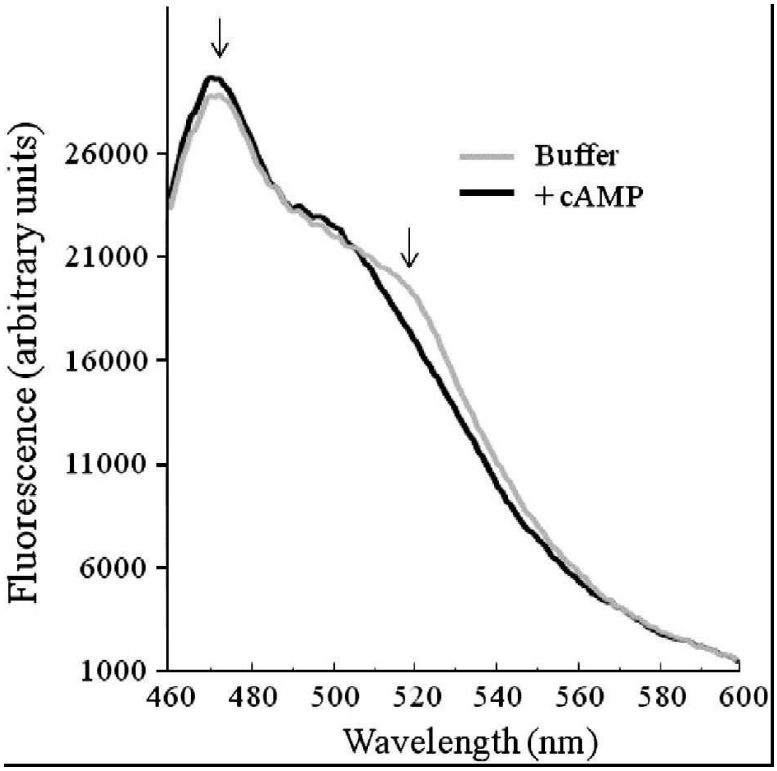

FIG 6.

Emission spectra of wild-type cells. Wild-type cells expressing Gα2-CFP and Gβγ-YFP (WT-FRET) were starved and then treated with buffer or cAMP. The cells were excited at 435 nm, and the emission spectrum recorded between 460 nm and 600 nm. These are representative scans of 20 – 25 individual experiments.

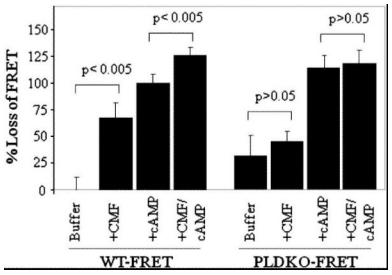

FIG 7.

Loss of FRET in wild-type and *pldB*$^{-}$ cells. Wild-type (WT-FRET) and *pldB*$^{-}$ (PLDKO-FRET) cells expressing Ga2-CFP and Gbg-YFP were starved and then treated with buffer, CMF, cAMP or both CMF and cAMP. The cells were excited at 435 nm, and the emission spectrum recorded between 460 nm and 600 nm. The amount of FRET was determined by taking the peak intensity ratio of donor CFP and acceptor YFP at 471 nm and 525 nm, respectively. The percentage loss of FRET was determined be setting the ratio of intensity for untreated WT-FRET cells at 0% and, WT-FRET cells in presence of cAMP at 100%. The results are the means of 20 – 25 individual measurements ± SEM.

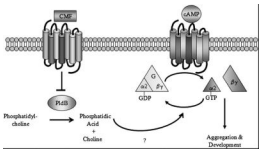

FIG 8.

Proposed mechanism for CMF signal transduction. CMF binds to its receptor, and inhibits PldB. This could be through the known CMF pathway involving Gα1βγ, and PLC, or through an as yet unidentified pathway. Decreased PldB activity decreases phosphatidic acid production and increases the dissociation between Gα2 and G βγ, most likely through inhibiting the Gα2 GTPase activity. This allows cAMP signaling and thus aggregation to occur.

Table 1

Effect of phosphatidic acid (PA) on low cell density aggregation.

Cell type and treatment	Presence of aggregates at cell density (× 10^3 cells/cm^2) of:					
	224	112	56	28	14	7
Ax2	+	+	+	+	−	−
Ax2+5 μM PA	+	+	−	−	−	−
Ax2+25 μM PA	+	−	−	−	−	−
Ax2+50 μM PA	−	−	−	−	−	−
pldB $^-$	+	+	+	+	+	+
pldB$^-$+5 μM PA	+	+	+	+	+	−
pldB$^-$+25 μM PA	+	−	−	−	−	−
pldB$^-$+50 μM PA	−	−	−	−	−	−

Wild-type Ax2 cells and *pldB*$^-$ cells were starved at various cell densities in submerged monolayer culture in the absence or presence of PA. The field of cells was then examined with an inverted microscope at 22 hours. The presence of aggregates is represented by a plus sign, while the absence of aggregates is represented by a minus sign. These are the representative results of three separate assays.